Received: 20 October 2022 | Revised: 30 May 2023 | Accepted: 27 August 2023

DOI: 10.1002/tox.23967

RESEARCH ARTICLE

ENVIRONMENTAL TOXICOLOGY WILEY

Exploring the mechanism of lung injury induced by lunar dust simulant in rats based on metabolomic analysis

Chen Gu[1] | Yuhang Yin[1] | Yan Sun[2] | Jinguo Liu[3] | Xiongyao Li[4] | Xiaoping Zhang[5]

[1]College of Basic Medical Sciences, Shenyang Medical College, Shenyang, China

[2]College of Pharmacy, Shenyang Medical College, Shenyang, China

[3]State Key Laboratory of Robotics, Shenyang Institute of Automation, Chinese Academy of Sciences, Shenyang, China

[4]Center for Lunar and Planetary Sciences, Institute of Geochemistry, Chinese Academy of Sciences, Guiyang, China

[5]State Key Laboratory of Lunar and Planetary Sciences, Macau University of Science and Technology, Taipa, China

Correspondence
Yan Sun, College of Pharmacy, Shenyang Medical College, Shenyang 110034, China.
Email: inksun@163.com

Funding information
Doctoral Scientific Research Fund of Liaoning Provincial Science and Technology Department, Grant/Award Number: 20198023; MUST-Partner Laboratory of Key Laboratory of Lunar and Deep Space Exploration, CAS, Grant/Award Number: 119/2017/A3; Open Projects Funding of Lunar and Planetary Science Laboratory; Science and Technology Development Fund (FDCT) of Macau, Grant/Award Number: 0014/2022/A1; Science and Technology Research Fund of Shenyang Medical College, Grant/Award Number: 20191017

Abstract

Inflammatory response and oxidative stress are considered to be important mechanisms of lung injury induced by lunar dust. However, the pulmonary toxicological mechanism remains unclear. In the present study, Wistar rats were exposed to CLDS-i 7 days/week, 4 h/day, for 4 weeks in the mouth and nose. Lung tissue samples were collected for histopathological analysis and ultra-performance liquid chromatography–mass spectrometry analysis. Enzyme activities and expression levels of key metabolic enzymes were detected by biochemical analysis and real-time PCR. The pathological features of lung tissue showed that CLDS-i caused congestion and inflammation in the lungs, and the lung structure was severely damaged. Metabolomics analysis showed that 141 metabolites were significantly changed in the lung tissue of the CLDS-i group compared with the control group. Combined with Kegg pathway analysis, it was found that the changes of amino acid metabolites were involved in these pathways, indicating that the simulated lunar dust exposure had the most obvious effect on amino acid metabolism in the lung tissue of rats. Real-time PCR analysis showed that the mRNA expression of six key enzymes related to amino acid metabolism was changed, and the enzyme activities of these key enzymes were also changed, which were consistent with the results of qPCR. These results suggest that changes in amino acid metabolism may be closely related to the pathogenesis of lung injury induced by lunar dust, and amino acid metabolism may be a potential biomarker of lung diseases related to lunar dust exposure.

KEYWORDS
amino acid metabolism, differential metabolites, lunar dust simulant, metabolomics, pulmonary toxicity

1 | INTRODUCTION

Lunar dust particles are the tiny particles covered on the lunar surface. Due to the charged nature of the lunar dust particles and the effect of the electric field around them. They easily suspend in the air. When the astronauts probe the lunar surface, these dust particles will stick to the helmets, space suits, and boots, making the astronauts' vision unclear and inconvenient to move. In addition, such particles with irregular shape and extremely complex structure will also cause wear and tear on space suits and detection equipment, posing a huge challenge to human landing on the moon. Studies have shown that exposure to lunar dust can cause a variety of adverse health effects, such as chronic bronchitis, chronic fibrosis of lung tissue, cardiovascular disease, skin inflammation, and conjunctivitis.

Due to the scarcity of real lunar dust samples, simulated lunar dust samples are currently used to study the toxicity of lunar dust

particles. Studies have shown that exposure of lunar dust simulated samples to the lungs caused local and systemic inflammatory responses in rats, significantly increased parasympathetic nerve activity, aggravated myocardial fibrosis, and ultimately led to myocardial dysfunction and cardiovascular damage.[1] The mechanism of cardiotoxic damage involves inflammatory mechanism, considering that NOX4 may be a potential therapeutic target of lunar dust simulant (LDS) induced myocardial injury.[1] Lam et al. studied the pulmonary acute toxicological effects of lunar dust simulants in mice and found that lunar dust was more toxic than titanium dioxide, but less toxic than silica-containing quartz dust.[2] Compared with the low-dose lunar dust group, the lung tissue of mice in the high-dose lunar dust simulant group showed mild to moderate alveolitis, as well as perivascular and peribronchiolar inflammation; after 90 days of exposure, the lung tissue showed mild Chronic lung inflammation, septal thickening, and some signs of fibrosis.[3] Stained sections of rat lung tissue exposed to simulated lunar dust showed different degrees of inflammatory lesions and fibrosis under microscope.[4] These results suggest that with prolonged exposure to simulated lunar dust and increasing doses, acute inflammatory responses in animals' lungs can be transformed into chronic inflammatory lesions in a dose-time-dependent manner. Sun et al. exposed rats to two doses of lunar dust simulant by tracheal instillation, and measured related immune and oxidative indicators in bronchoalveolar lavage fluid (BALF) of rats. The results confirmed that under the effect of simulated lunar dust, inflammation, oxidative stress and immune response promote each other, causing pulmonary vascular endothelial cell damage and lung inflammation, and inducing lung injury.[4–6] However, the pathogenesis of lung injury induced by simulated lunar dust has not been clearly elucidated. Therefore, more in-depth studies are needed to better understand the pathogenic process of lunar dust simulants exposure leading to pulmonary toxicity.

Metabolomics reveals the dynamic changes of various metabolites caused by the pathological state of the living system by analyzing the changes of metabolites after the biological system is stimulated by external factors, describing the phenotype of the organism and studying the pathological mechanism of the occurrence and development of diseases.[7] In the PM2.5 exposure study, some scientists found that the lung metabolome of rats exposed to PM2.5 for a long time changed significantly. Combined with the results of oxidative stress, PM2.5 can induce pulmonary toxicity by disturbing the pro-oxidative/anti-oxidative balance.[8] Metabolomics analysis showed that its differential metabolites were mainly involved in the citric acid cycle, glyoxylate and dicarboxylic acid metabolism, pyruvate metabolism, purine and pyrimidine metabolism, and valine, leucine and isoleucine metabolism and other pathways.[7] When nuclear magnetic resonance (NMR)-based metabolic methods were used to study the changes in the metabolic components of A549 cells treated with PM2.5, 12 metabolites were significantly changed, and the related metabolic pathways involved are similar to the results of Li et al., mainly involving amino acid metabolism, lipid metabolism, nucleotide metabolism, and the tricarboxylic acid cycle.[9] In addition, in experiments with pregnant mice, the mRNA levels of the inflammatory mediator Pla2g2d and its metabolites lysophosphatidylcholines (LysoPCs) and arachidonic acid (AA) were up-regulated in the lung tissue of PM2.5 group, by contrast, these inflammatory changes were recovered after treatment with mogrosides (MGs) during pregnancy; Pla2g2d was suggested to be a potential target of MGs to ameliorate PM2.5-induced lung injury.[10] These studies all confirm that metabolomic approaches are effective tools to characterize metabolic changes in air pollution-induced lung injury.[11] Lunar dust, as the fine dust particles existing on the lunar surface, has a lung toxicity far greater than that of PM2.5 due to its special physical and chemical properties. In the past, studies on lung injury induced by lunar dust simulant did not focus on the metabolomics study of lung tissue, and the relationship between lunar dust simulant exposure and metabolites in lung tissue was unclear. Therefore, this study was based on metabolomic analysis of metabolite changes in the lung tissue of simulated lunar dust-exposed rats to search for potential biomarkers to reveal its underlying pathogenesis.

2 | MATERIALS AND METHODS

2.1 | Preparation of simulated lunar dust suspension

The simulated lunar dust sample CLDS-i used in this study was developed by the Institute of Geochemistry, Chinese Academy of Sciences. The researchers further processed the simulated lunar dust sample CLRS-1 developed earlier, and obtained CLDS-i, which is very similar to the real lunar dust in terms of mineral composition, physicochemical properties, grain size and nano-metal iron properties. Most of the particles in CLDS-i are less than 1 μm in diameter.[6] After autoclaving, vacuum freeze-drying, and store at −80°C. Preparing simulated lunar dust suspension with normal saline for use.

2.2 | Animal protocol

Twenty-eight healthy SPF grade male Wistar rats, weighing 190–220 g were obtained from Beijing Huafukang Biotechnology Co. Ltd. (Animals License number: SCXK [Jing] 2019–0008). They were placed in polycarbonate cages (equipped with HEPA air filters), 2 animals/cage, 12 h-12 h light/dark cycle, room temperature: 24°C ± 2°C, relative humidity: 50% ± 5%, with free access to food and water, and were reared for 1 week to observe their activities and feeding. Then they were weighed and randomly divided into two groups: simulated lunar dust group and normal saline control group, with 14 animals in each group.

The Wistar rats in the experimental group were placed in the oral and nasal exposure chamber (Beijing Huironghe Technology Co., Ltd.) to be exposed to dust at a concentration of 7 mg/m^3 CLDS-i for 4 h/d, 7 d/week for 4 weeks, and the control group was exposed to normal saline under the same conditions. In accordance with the requirements of inhalation toxicity Testing guidelines issued by the Organization for Economic Co-operation and Development (OECD), The system Settings are as follows: aerosol flow rate: 2 L/min, dilution

flow rate: 43 L/min, extraction flow rate: 44 L/min, preset concentration: 7 mg/m3, upper temperature limit: 25°C, lower temperature limit: 19°C, upper humidity limit: 70%, Lower humidity limit: 30%, upper concentration of O_2: 25%, lower limit of O_2 concentration: 19%, upper limit of CO_2 concentration: 1.0%, lower limit of CO_2 concentration: 0.0%.[12] Rats were sacrificed 1 week after the last exposure for the next step of the experiment. Animal experiments were performed in accordance with the guidelines of the Animal Experiment Center of Shenyang Medical College, and all animal studies were approved by the institution's animal research ethics committee.

2.3 | Histopathological examination

Partial bilateral lung tissue (unwashed) of each group of rats was taken and stored in containers with 10% paraformaldehyde solution for at least 7 days, then dehydrate in ethanol gradients, xylene transparent treatment, paraffin-embed tissue and section at 5 μm, followed by optical staining with hematoxylin and eosin (H&E) Microscope observation.

We performed a semi-quantitative analysis of alveolar inflammation in each group of rats. The scoring method is based on Szapiel et al., 0 score: no alveolar inflammation; 1 score: No widening of alveolar septum, monocyte infiltration, complete alveolar structure, lesions <20%; 2 scores: the inflammation was more extensive, and the lesions reached 20%–50%; 3 scores: Lesions >50%, occasional consolidation and vesicles, monocyte infiltration and bleeding areas in alveolar cavities or alveolar Spaces.[13]

2.4 | Pulmonary metabolome analysis

Lung tissue samples of rats in the normal saline control group ($n = 6$) and the CLDS-i group ($n = 6$) were collected and homogenized respectively, and 400 μL of pre-cooled methanol/acetonitrile/water solution (4:4:2, v/v) was added. Vortex mixing, let stand at −20°C for 60 min, centrifuge at 14000×*g* for 20 min at 4°C, take the supernatant and vacuum dry, add 100 μL of acetonitrile aqueous solution (acetonitrile: water = 1:1, v/v) for reconstitution during mass spectrometry analysis, Vortex, centrifuge at 14000×*g* at 4°C for 15 min, and take 2 μL of the supernatant for ultra-high performance liquid chromatography-mass spectrometry (UPLC-MS, Thermo Fisher Scientific, USA) analysis.

UPLC-MS raw data was imported into Compound Discoverer 3.2 (Thermo Fisher Scientific, USA) software for processing, and obtained a table containing metabolic features (m/z-retention time pairs) and peak intensities. Peak detection, retention time correction and alignment were performed using the following parameters: mass range 70–1050 *m/z*, peaks finding method centWave, mass tolerance 10 ppm, and retention time (RT) width threshold 40s. All extracted features were normalized to total intensities to eliminate systematic bias. The features with missing values in >50% of the samples were excluded. Corresponding to the missing values, select fill gap in the software to fill the missing values. Unit variance scaling was performed on the processed tables, and then imported to SIMCA-P 14.1 software (Umetrics, Umea, Sweden) for univariate and multivariate statistical analysis. Univariate analysis methods, including Student's *t*-test and fold-of-variation analysis, were used to visually display the difference between the two groups of samples. Multivariate statistical analysis was then performed, including unsupervised principal component analysis (PCA), supervised partial least squares discriminant analysis (PLS-DA) and orthogonal partial least squares discriminant analysis (OPLS-DA). According to the variable importance for the projection (VIP) obtained by the OPLS-DA model, p-value < .05 and VIP > 1 were used as the screening criteria to mine biologically significant differential metabolites. Volcano, column, and heat maps were constructed to visualize differences in metabolite levels for each comparison.[10] Subsequently, the Kyoto Encyclopedia of Genes and Genomes (KEGG) pathway enrichment analysis and correlation network analysis were performed for the significantly differential metabolites.

2.5 | RNA isolate and quantitative real-time PCR analysis

According to the manufacturer's instructions, from the remaining frozen lung tissue, total RNA was extracted with TRIzol reagent (Vazyme, China), and the isolated RNA was converted into cDNA using HiScript IIQRT SuperMix for qPCR(+gDNA wiper) reverse transcription reagent (Vazyme, China), qPCR reactions were performed in an ABI PRISM 7500 system. The mRNA expression of glutathione sulfur transferase (GST), glutamate decarboxylase (GAD), glutamate dehydrogenase (GDH), α-ketoglutarate dehydrogenase (OGDH), glutaminase (GLS) and ornithine decarboxylase (ODC) was measured by real-time quantitative polymerase chain reaction (qPCR) using SYBR Green PCR Master Mix (Vazyme, China), with the housekeeping gene β-actin as an internal PCR control. The forward primers and reverse primers (Invitrogen, CA, USA) were summarized in Table 1. Data were analyzed using the comparative threshold cycle (CT) method, performed in triplicate for each set of samples. The reaction conditions were as follows: an initial denaturation step at 95°C for 30 s; followed by 40 cycles in a cycling reaction of 10 s at 95°C and 31 s at 60°C. The fold changes of the tested genes were analyzed using the $2^{-\Delta\Delta CT}$ method.

2.6 | Biochemical analysis

Enzymatic activities of GST, GDH and GAD in the two groups of samples were detected using the biochemical assay kit (Jiangsu Addison Biotechnology Co., Ltd., Jiangsu, China). Elisa Kit (Shanghai Yuanju Biotechnology Center, Shanghai, China) detects GLS, ODC and OGDH. The specific experimental procedure is as follows. The specific

TABLE 1 The forward and reverse primers used in this study.

Gene names	Forward primers	Reverse primers
GST	CGAAAGCTTTGCAACAATCGC	GCATTAGAAAACGTGTTGGCCT
GAD	GCTGGAAGGATGGAAGGTTTTAA	AATATCCCATCACCATCTTTATTTGACC
GDH	ATCCTGCGGATCATCAAGCC	GCACCTCCAAATGGCACATC
OGDH	TACCCACCACCACTTTCAT	CCAGCAGGGTCCGCTTCTCC
GLS	AATGCACTCCTGTGGCATGT	AAGGAATGCCTTTGATCACCTC
ODC	CCTGTGCTGTGAGGAGACAG	ACACGGGGAAGAGCTTTCAG
β-Actin	GCTCTCTTCCAGCCTTCCTT	AATGCCTGGGTACATGGTGG

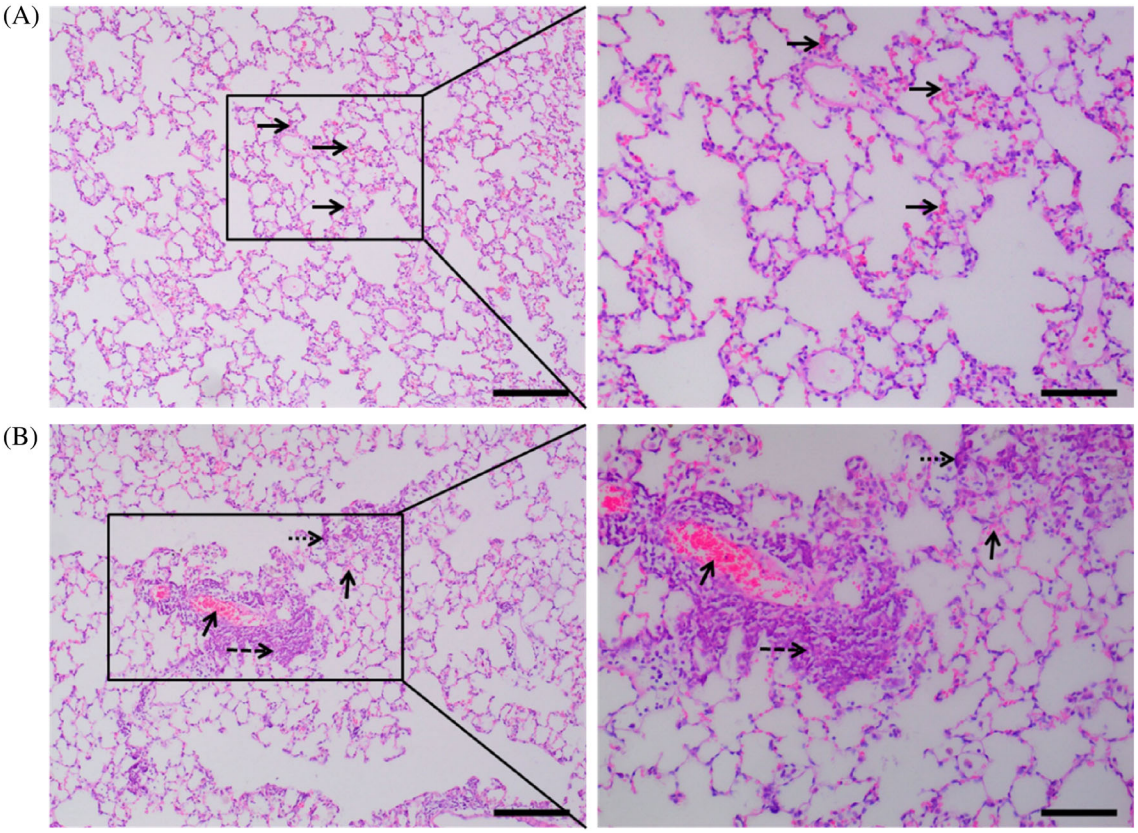

FIGURE 1 Hematoxylin–eosin-stained histopathological pictures of rat lungs. (A) saline group. (B) CLDS-i group. The lung structure of saline group was basically normal. → = the alveolar wall was slightly congested in the saline group. ➡ = a large number of the inflammatory cells in CLDS-i group. ⇢ = the obvious thickening pulmonary interstitial in CLDS-i group. → = the hyperemia was more severe in CLDS-i group. Original magnification × 100; scale bar = 200 μm left, original magnification × 200; scale bar =100 μm right.

experimental procedure should be operated according to the kit instruction.

2.7 | Statistical analysis

All data were analyzed by SPSS 20.0 statistical software and expressed as mean ± SD. Statistically significant differences were assessed using *t*-test and one-way analysis of variance (ANOVA) for multiple comparisons between groups. $p < .05$ was defined as a statistically significant difference.

3 | RESULTS

3.1 | Pathological changes in rat lung tissues

H&E staining was used to observe the pathological changes of lung tissue after CLDS-i exposure. Results of H&E staining showed that in the control group, the lung structure was basically normal. The alveolar size was basically normal, and the alveolar wall was mildly congested (Figure 1A). In the CLDS-i group, more severe hyperemia was observed, with numerous lymphocyte and neutrophil aggregates and infiltrates accompanied by marked septal thickening. The alveolar

structure changed significantly, and the basic structure of some parts of the lung was unclear (Figure 1B). Semi-quantitative analysis results are shown in the Table 2 below. The score of alveolar inflammation in CLDS-i group was significantly higher than that in saline control group ($p < .01$), indicating that the lung inflammation in CLDS-i group was aggravated.

TABLE 2 Comparison of scores of alveolar inflammation in each group ($n = 5$, $\bar{x} \pm s$).

Group	*n*	Scores
NS	5	1.4 ± 0.55
CLDS-i	5	3.0 ± 0.0**

Note: Compared with the saline control group.
**$p < .01$.

3.2 | Pulmonary metabolomics analysis

Rat lung samples were detected by UPLC-MS analytical method, and PCA analysis (Figure 2) and PLS-DA analysis (Figure 3) were performed to describe the overall metabolomics differences of rat lung tissue samples in each group. PCA is one of the earliest and widely used multivariate pattern recognition methods for preliminary analysis of MS datasets. Figure 2 is a graph of the scores of PCA in positive and negative ion mode. The *x*-axis and *y*-axis in the figure represent the first principal component and the second principal component after dimension reduction of the PCA algorithm, respectively. Icons in different colors represent experimental and control groups. Among them, the red dots represent 6 CLDS-i-treated rat lung samples, and the blue triangles represent 6 saline-treated lung samples. Figure 3 is a graph of the scores of PLS-DA in positive and negative ion mode. PLS-DA is a supervised pattern recognition method, which can achieve better classification results compared with PCA. After

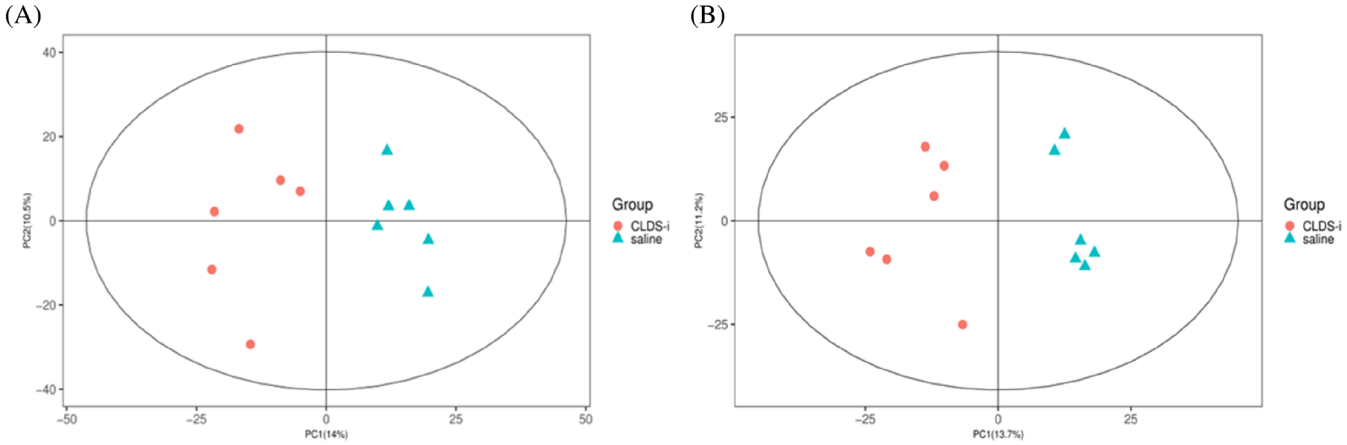

FIGURE 2 The PCA score map of the metabolic profile of rat lung tissue was drawn in the positive ion mode (A) and negative ion mode (B).

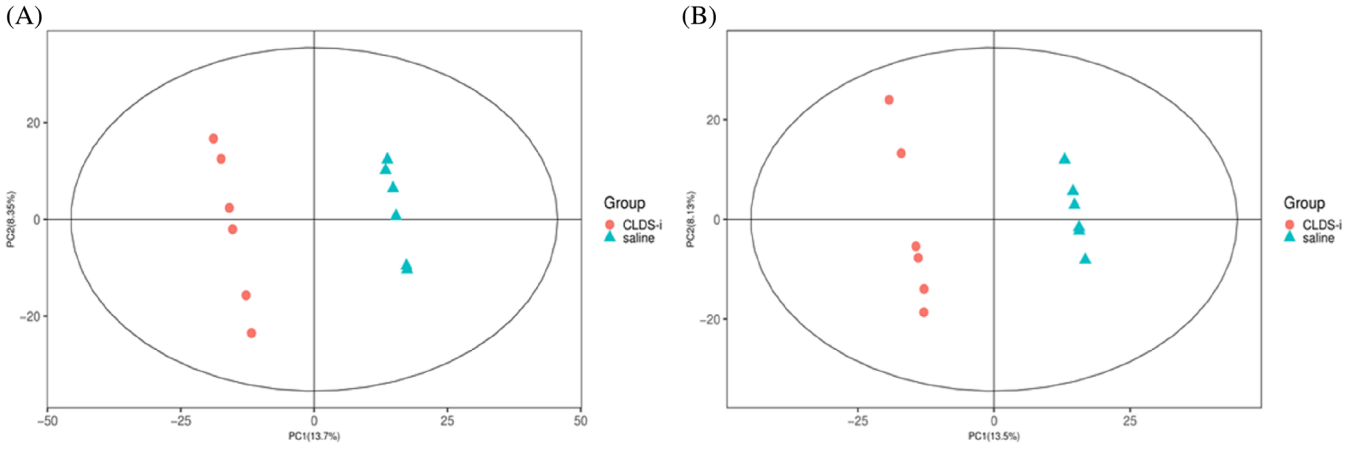

FIGURE 3 Analysis of metabolite profiles using PLS-DA model. Multivariate statistical analysis of different rat lung tissue metabolites from the saline group (▲) and CLDS-i group (●). PLS-DA score plot from the ESI positive ion mode (A) and negative ion mode (B).

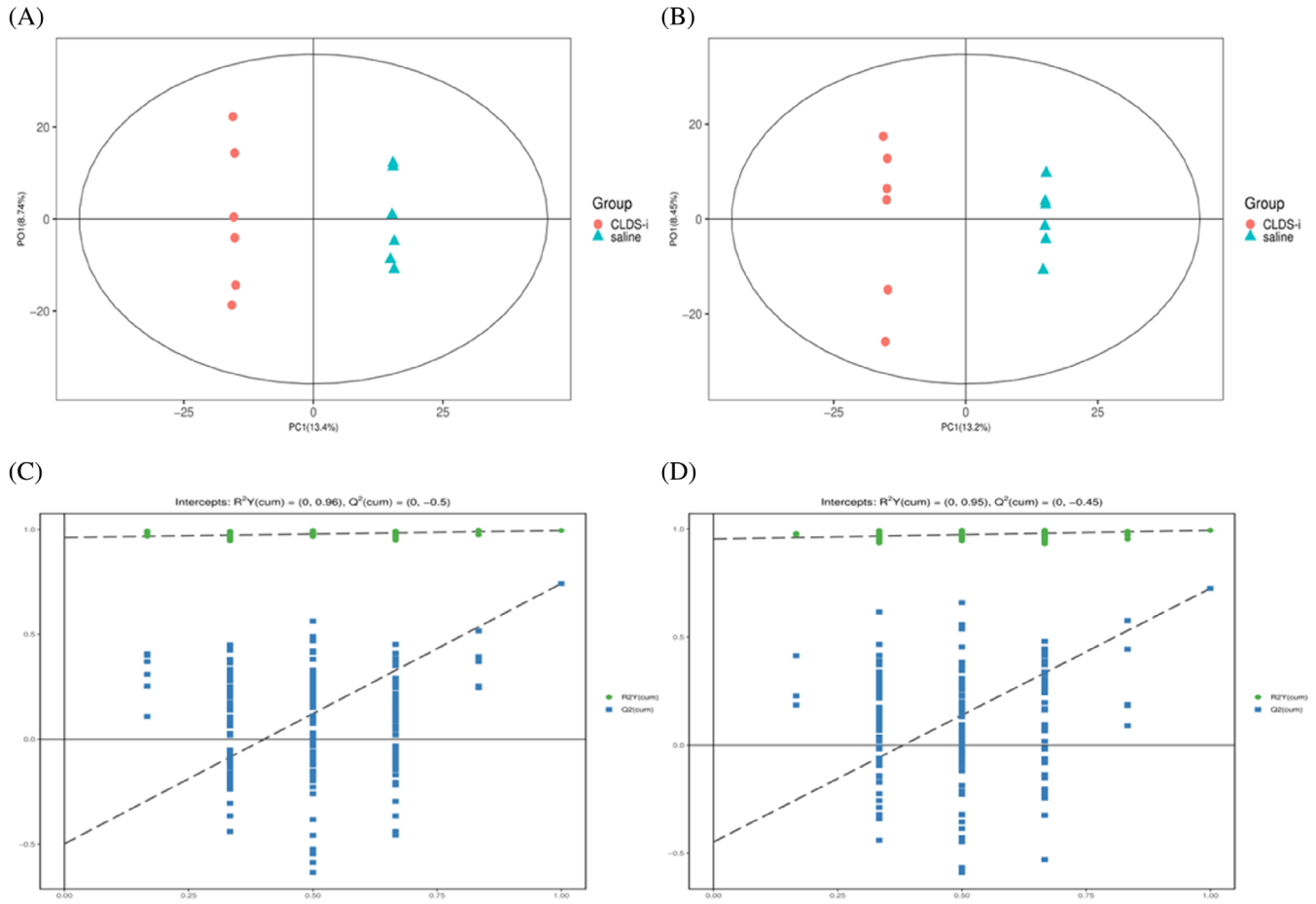

FIGURE 4 OPLS-DA score plots and permutation tests between two groups in rat lung tissue. (A) OPLS-DA score plots of control and experimental groups (ESI (+)). (B) OPLS-DA score plots of control and experimental groups (ESI (−)). (C) The result of the permutation test made of OPLS-DA (ESI (+)). (D) The result of the permutation test made of OPLS-DA (ESI (−)).

calculation by PCA and PLS-DA algorithm, sample points within each group showed obvious aggregation, while CLDS-i group was significantly separated from the saline group. It indicated that CLDS-i exposure induced disturbance of lung metabolites.

In order to obtain a more significant effect of metabolite separation between groups, we used the OPLS-DA model for analysis. A and B in Figure 4 are the score of the OPLS-DA in the positive and negative ion mode of the two groups of lung tissues, respectively. As a result, after calculation by the OPLS-DA algorithm, the sample points of each group were clustered obviously, and the CLDS-i group and the control group were scattered in two different areas, and the separation effect was good, which further confirmed that CLDS-i caused the disorder of metabolites in lung tissue of rats.

Figure 4C, D show the permutation test plots performed by the OPLS-DA model based on positive and negative ion mode data. The permutation test was used to evaluate the fitting ability and prediction ability of the model established by OPLS-DA. The principle of permutation test is to rearrange the samples and rebuild a new model. Each permutation test presents a set of model-dependent parameters R2 and Q2. The green dots (R2) represent the fitting ability of the model, and the blue boxes (Q2) assess the predictive ability of the model. The current criterion for model validity is that the regression line at Q2 intersects the vertical line below zero.[14] In our study, the values of R2 and Q2 were ≥0.5, and the results met the above criteria, indicating that the fitting ability of the model was in good agreement with the predictive ability.

We used the fold change (FC) of metabolite expression difference between the two groups of samples and the *p*-value obtained by the *t*-test to draw the volcano plot to show the significant difference between the two groups of sample data. The abscissa is the fold difference $\log2^{FC}$, which represents the log2 of the fold change of metabolites between the two groups. The ordinate is the significance of the difference −log10P, representing the −log10 of the *p*-value of the t-test for the metabolites between the two groups). We used the "q-value" package in the R platform (http://www.r-project.org) to map the p-value of each t-test to the q-value of Storey Tibshirani to estimate the false discovery rate (FDR) of the test when it's called significant. The following criteria are used for preliminary screening of differential metabolites: fold change ≥2 or ≤0.5; *p*-value < .05; false discovery rate (FDR) ≤0.2.[15] The red dots in the figure are significantly up-regulated metabolites, the blue dots are significantly down-regulated metabolites, and the gray dots are metabolites with no

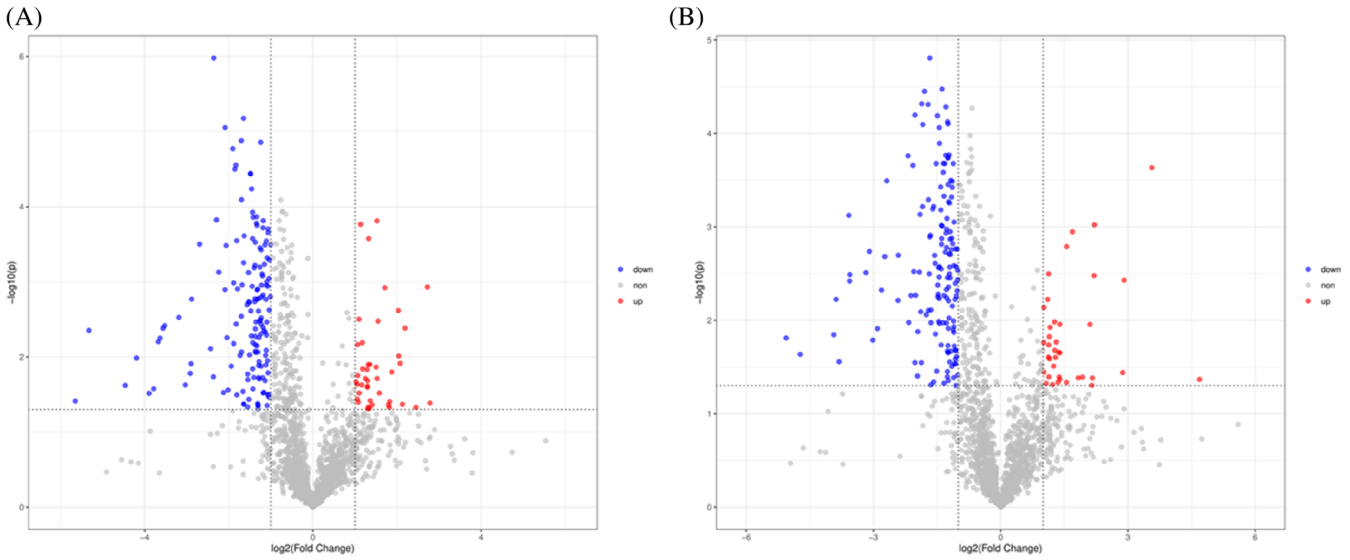

FIGURE 5 Differential changes of metabolites in lung tissue of two groups of rats are shown by volcano plots. (A) The results in the ESI positive ion mode. (B) The results in the ESI negative ion mode.

significant difference. It can be seen from Figure 5 that there are a large number of significantly different metabolites in the lung tissue of the CLDS-i group and the control group.

In order to screen out more significant differential metabolites, variable importance in projection (VIP) obtained by the OPLS-DA model was used to measure the impact strength and explanatory power of the expression pattern of each metabolite on the classification and discrimination of each group of samples. Using p-value < .05, false discovery rate (FDR) ≤ 0.2 and VIP > 1 as the screening criteria. Significant differences in compounds with biological significance were mined. A total of 141 differential metabolites were identified between the CLDS-i group and the control group, and the fold change (FC) heat map was drawn according to the metabolite type, and it was found that these metabolites were involved in the metabolism of lipids, amino acids, carbohydrates and nucleotides (Figure 6). Its results were consistent with those of the network analysis (Figure 7) constructed between the significantly different metabolites. It was shown that the simulated lunar dust particles-CLDS-i led to the change of the whole metabolic profile of the rat lung tissue, and metabolic changes were not singly occurred, and the differential metabolites interacted and connected with each other. Compared with the control group, the CLDS-i group had decreased levels of most metabolites, including D-(−)-aspartic acid, L-glutamic acid, asparagine, glutamine, L-(+)-Proline, L-Histidine, L-Valine, L-leucine, Tryptophan, lysine, Taurine, arginine, D-pantothenic acid, spermidine, putrescine, glutathione, PG(18:1(11Z)/18:2(9Z,12Z)), choline, docosahexaenoic acid, xanthine, uric acid, cytosine, uracil, and so on.

To comprehensively and intuitively display the relationship between samples and the differences in the expression patterns of metabolites in different samples, we performed hierarchical clustering of each group of samples using qualitatively significant differential metabolite expression levels. Figure 8 is a hierarchical clustering heat map analysis between the experimental group and the control group. The right and top of the figure are the names of the differential metabolites and the classification of the samples, respectively, each column represents the amount of different metabolites in the same sample, and each row represents the relative amount of the same metabolite in different samples. The more metabolites, the closer the color is to red; the less metabolites, the closer to blue. The dendrogram on the left represents different cluster analysis results for different samples. Two substances linked by cluster analysis were highly correlated. The hierarchical clustering analysis shown in the figure is statistically significant, therefore, we believe that the amount of expression of these metabolites is different between the two groups of samples, the color distribution within each group is similar, but the difference between groups is large, indicating CLDS-i affected the metabolomic characteristics of rat lung tissue.

To further analyze the metabolic pathways associated with the significantly differential metabolites, the differential metabolites were entered into the Kyoto Encyclopedia of Genes and Genomes (KEGG) database to construct and analyze the metabolic pathways. As showed in Figure 9, the top 10 metabolic pathways with the greatest impact were screened, namely protein digestion and absorption, central carbon metabolism in cancer, aminoacyl-tRNA biosynthesis, ABC transporters, biosynthesis of amino acids, alanine, aspartate and glutamate metabolism, mineral absorption, beta-alanine metabolism, Arachidonic acid metabolism and neuroactive ligand–receptor interaction. We further analyzed these metabolic pathways and observed that amino acid metabolite changes were involved in these pathways, indicating that simulated lunar dust exposure caused the most obvious changes in amino acid metabolism in rat lung tissue.

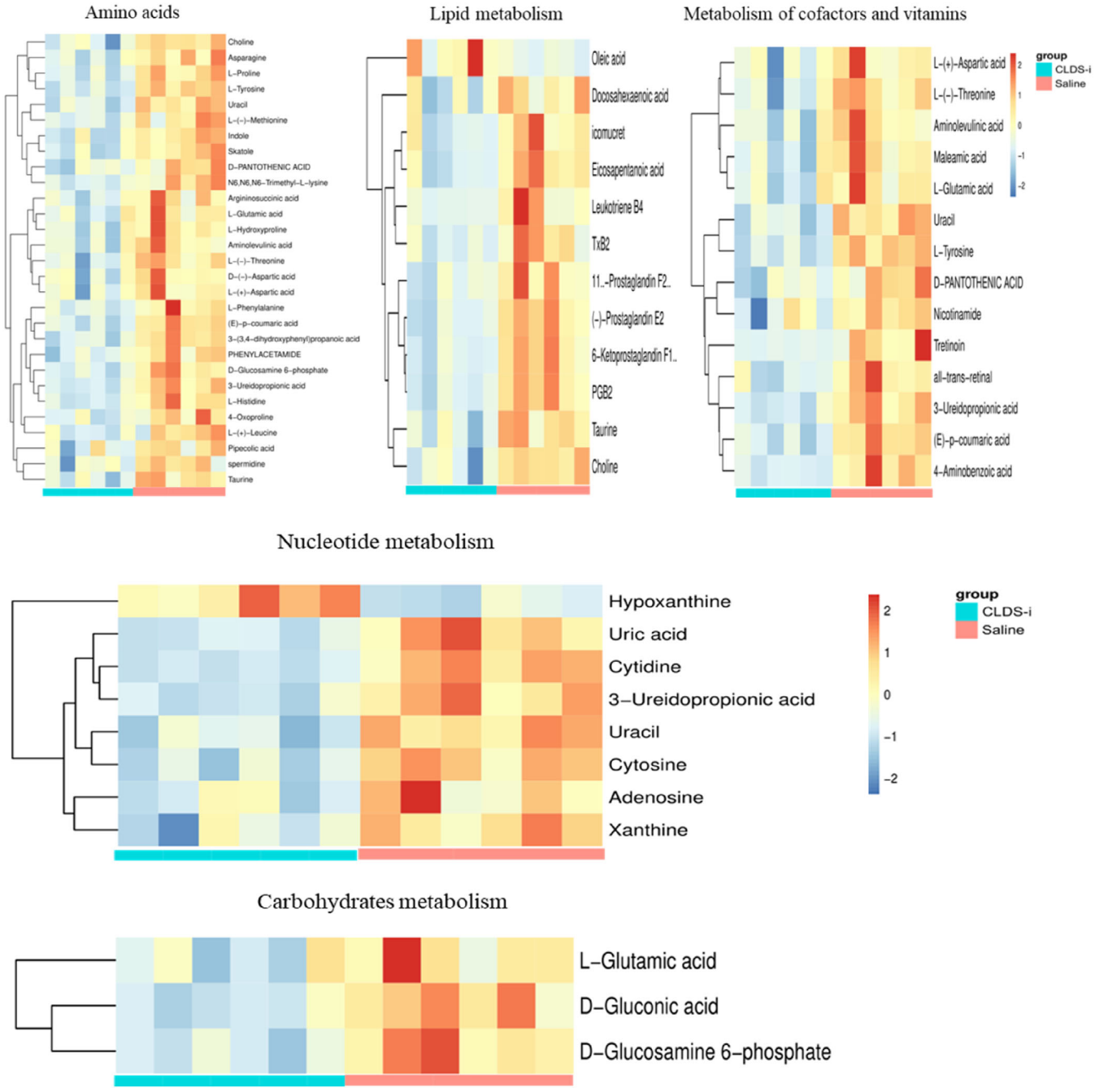

FIGURE 6 Differential fold heat map based on participating differential metabolite types.

3.3 | Gene expression differences of key enzymes related to amino acid metabolism in lung tissue

In order to further confirm the effect of simulated lunar dust particles CLDS-i on amino acid metabolism in rat lung tissue, we used qRT-PCR to detect the gene expression of key enzymes related to amino acid metabolism. The results are shown in Figure 10. Compared with the control group, the mRNA levels of GST, ODC, OGDH, GLS, and GDH in the CLDS-i group increased, while the mRNA level of GAD decreased ($p < .05$). These results indicate that the simulated lunar dust exposure disrupted amino acid metabolic homeostasis in rat lung tissue.

3.4 | Enzyme activity of key enzymes related to amino acid metabolism

In addition, we detected the enzymatic activities of GST, ODC, OGDH, GLS, GAD, and GDH, as showed in Table 3. Compared with the saline group, the enzymatic activities of GST, ODC, OGDH, GLS,

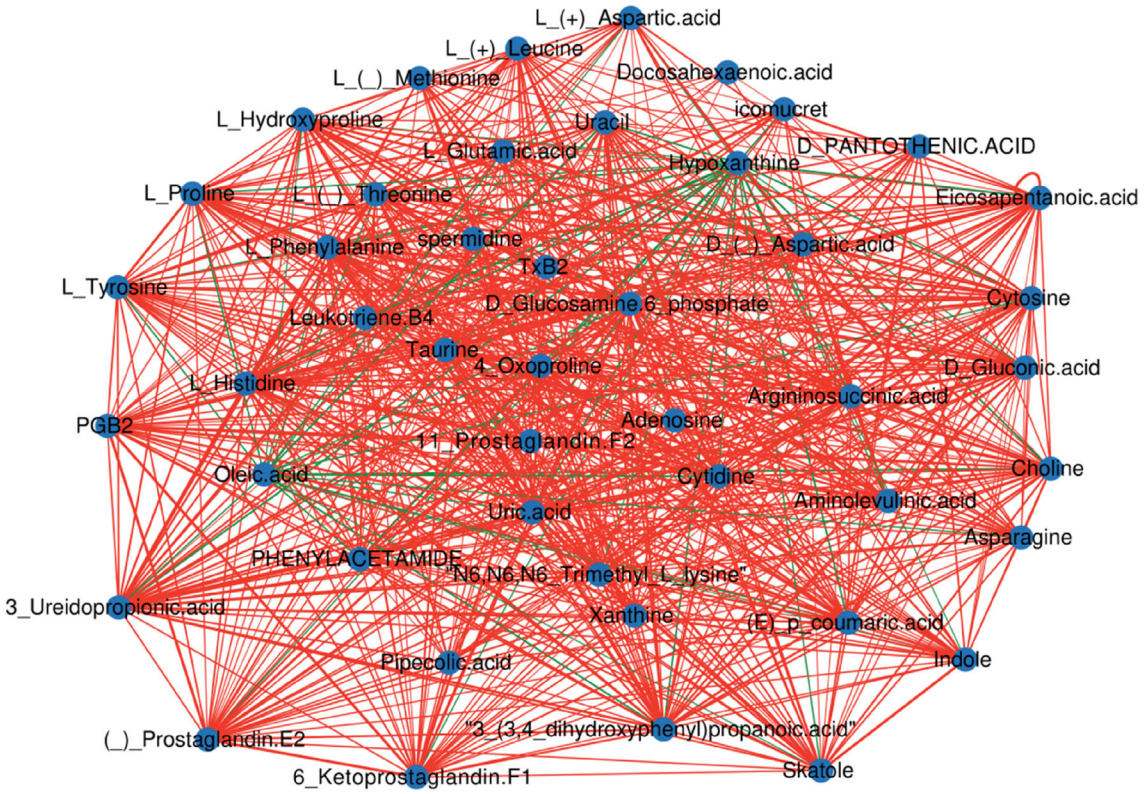

FIGURE 7 Correlation network of identified differential metabolites ($p < .05$, $r > .6$) calculated by Cytoscape 3.4.0. Red lines between differential metabolites indicate positive correlations, while green lines indicate negative correlations.

and GDH were significantly up-regulated in the CLDS-i group, while the enzymatic activity of GAD was down-regulated. The data indicated that CLDS-i exposure disrupted amino acid metabolic homeostasis in rat lung tissue.

4 | DISCUSSION

A growing number of studies have shown that exposure to lunar dust particles can adversely affect human health, which can increase the incidence of various diseases, especially lung diseases. It is generally believed that inflammatory response and oxidative stress are the main modes of action of lunar dust-induced lung injury.[6] However, the mechanism of lunar dust-induced lung injury is still unclear, and there are few studies on the interference of the fine particles on metabolites and metabolic pathways in lung tissue. This study aimed to elucidate the molecular toxicity mechanism of simulated lunar dust-induced lung injury in rats using UPLC-MS metabolomics approach. In the previous study, we mostly used the tracheal instillation method to create the model, but during the experiment, we found that this method is easy to cause mechanical damage to the tracheal mucosa of rats, bleeding, lung infection, and high mortality. Due to the non-physiological route of administration, this results in the deposition of particles of various sizes with the same spatial distribution, making the method limited.[6] Compared with the tracheal instillation method, the animal mortality rate of the inhalation method is lower, and it can reflect the pathological process more realistically. Therefore, in this study, we established a rat lung injury model through the oronasal exposure system.

The doses inhaled in rats in this study were determined based on data published by Lam et al.[16] No statistically significant differences in biomarkers were reported between rats exposed to two concentrations of lunar dust, 2.1 and 6.8 mg/m^3. 6.8 mg/m^3 was considered to be the highest no apparent adverse effect level (NOAEL). Rats exposed to 20 mg/m^3 for 4 weeks showed some minor effects but were larger than expected and produced mild to moderate pulmonary toxicity in the 60 mg/m^3 exposure group. Since the simulated lunar dust suspension was used in this experiment instead of dust particles, 7 mg/m^3 was chosen as the exposure concentration in this study, considering that it may have a greater impact on the lungs. And the concentration is not expected to cause an overdose.

Our results showed that a total of 141 metabolites were significantly altered in rat lung tissue exposed to simulated lunar dust, and these metabolites were involved in the disturbance of amino acid, lipid, and nucleotide metabolic balance. And we screened out the most significant 10 metabolic pathways and further analyzed them, and found that amino acid metabolism pathways have the greatest impact, for example, protein digestion and absorption, central carbon metabolism in cancer, aminoacyl-tRNA biosynthesis, ABC transporters, biosynthesis of amino acids, alanine, aspartate and glutamate

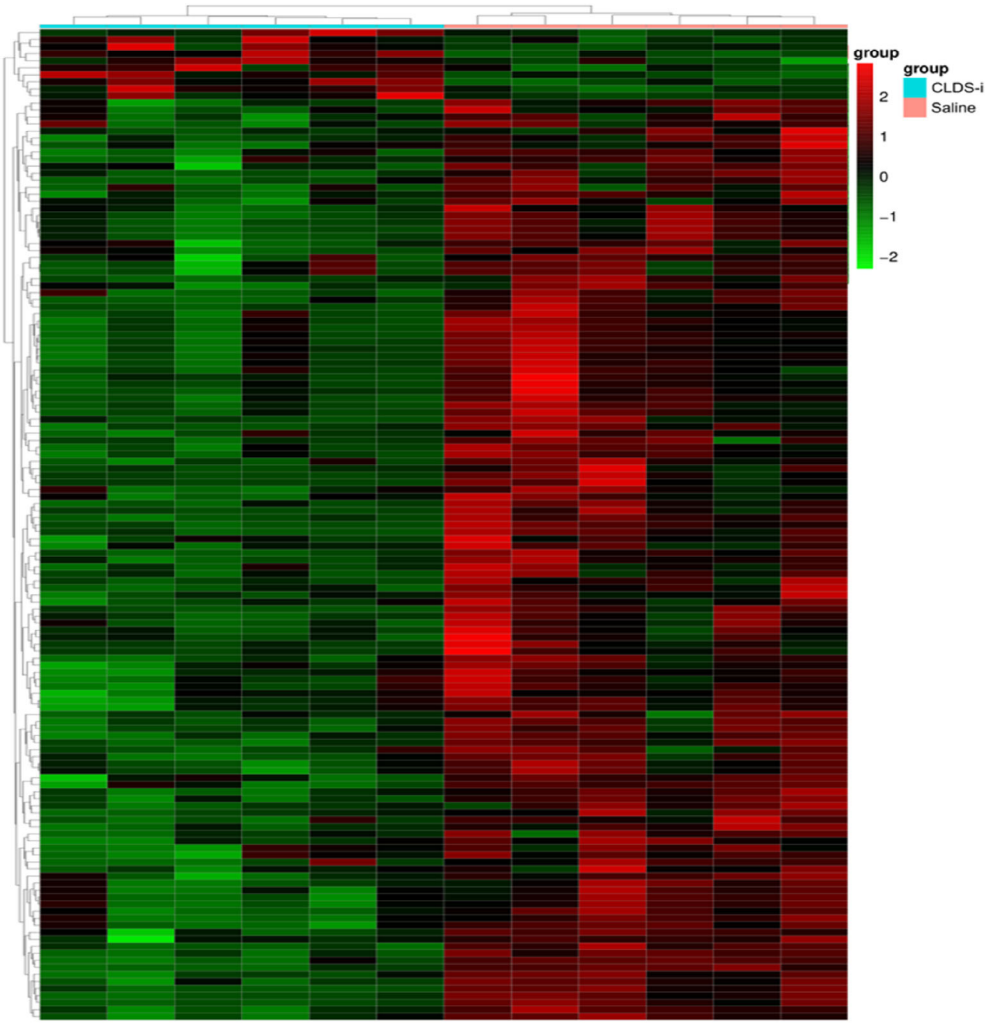

FIGURE 8 Hierarchical cluster heat map analysis of differential metabolites between control (Saline) and experimental group (CLDS-i).

metabolism, and mineral absorption. And these significantly changed amino acid metabolites play an important role in the regulation of immune function, the regulation of the body's oxidative-antioxidant balance and the reduction of inflammatory responses.

Amino acids are the building blocks of proteins and polypeptides in the human body and play important roles in energy generation, nucleoside synthesis and maintenance of cellular redox balance, and are involved in regulating key metabolic pathways necessary for growth, reproduction and immunity.[17] Amino acid metabolism involved in this study is extensive. Among them, glutamine is an amino acid that is abundant in animals, and its concentration in tissues and plasma is more than 10 times that of other amino acids.[18] In almost every cell, glutamine can be used as a substrate for nucleotide synthesis (purines, pyrimidines, and amino sugars), nicotinamide adenine dinucleotide phosphate (NADPH), antioxidants, and many other biosynthetic pathways involved in the maintenance of cellular integrity and function.[19–21] A large numbers of studies have confirmed that glutamine plays an important role in the body's anti-inflammatory. A study by Raizel et al. showed that chronic oral glutamine therapy following progressive resistance exercise (RE) promoted cytoprotective effects involving HSP70 responses. Thereby reducing muscle damage and inflammation.[22] In their study, Singleton et al.[23] observed that glutamine treatment can effectively inhibit the activation of NF-kBeta and the expression of cytokines in septic mice, and the tumor necrosis factor-alpha (TNF-α) and interleukin- 6 (IL-6) in lung tissue of mice were significantly reduced. Zabot et al[24] also found that glutamine can inhibit the positive expression of nuclear factor kappaB (NF-κB) and IL-6 in the intestinal ischemia/reperfusion (I/R) rat model, improve the activity of antioxidant enzyme SOD, and prevent mucosal damage, and improve intestinal and lung recovery after I/R injury in rats. This fully shows that glutamine affects the NF-κB signaling pathway and inhibits its activation, thereby inhibiting the expression of its downstream inflammation-related factors, so that the body's pneumonia inflammation can be alleviated. In addition, studies have shown that cells of the immune system, such as lymphocytes, neutrophils, and macrophages utilize glutamine at high rates similar to or higher than glucose under catabolic conditions such as sepsis, recovery from burns or surgery, malnutrition, and high-intensity/high-volume physical activity.[25,26] Therefore it considers to be "fuel for the immune system".[27] In immune cells, glutamine is converted to glutamate, aspartate, and alanine by partial oxidation to CO_2, and this unique conversion plays a key role in the efficient functioning of immune

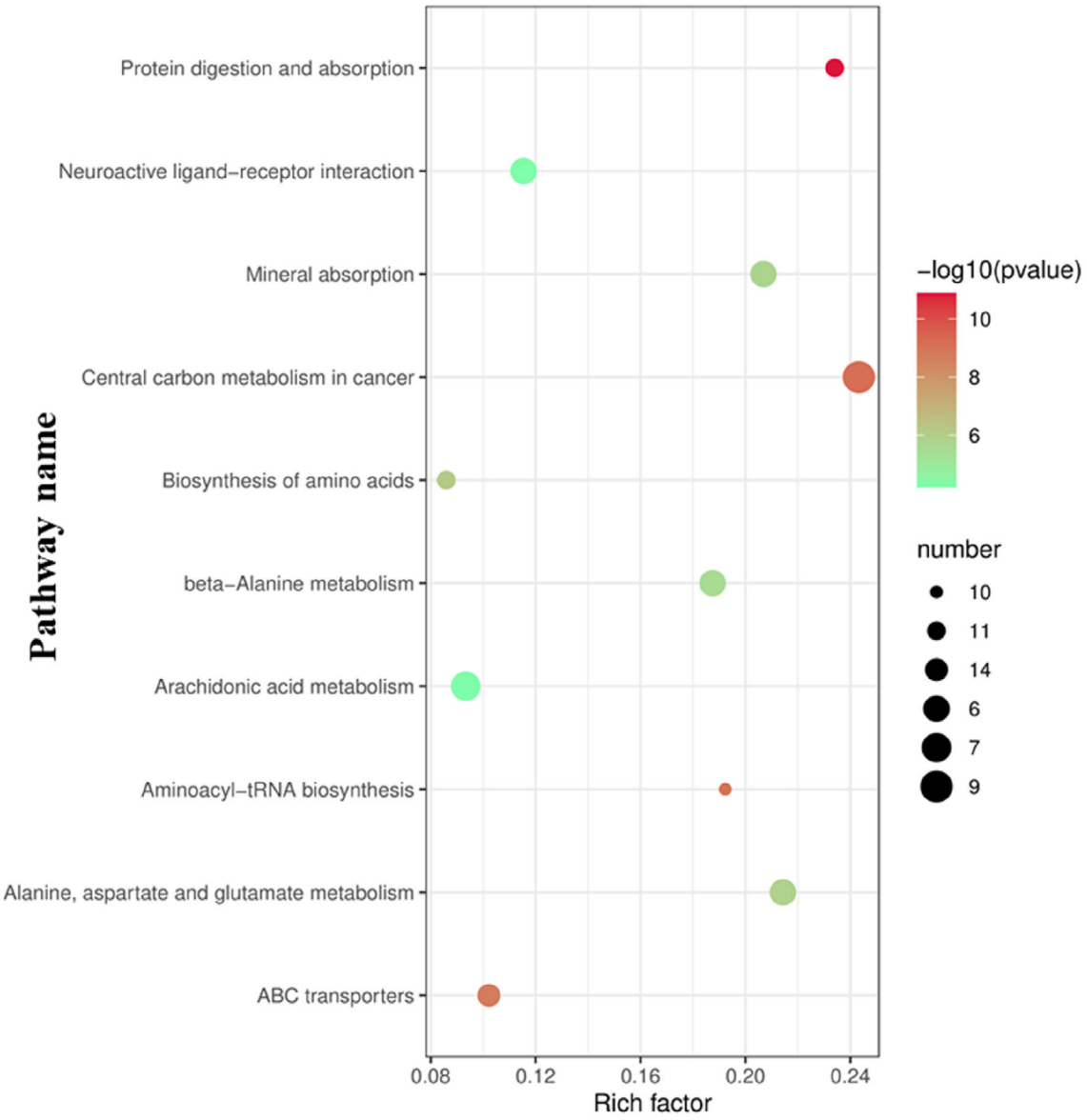

FIGURE 9 Analysis of relevant metabolic pathways for differential metabolites between exposing and control groups. KEGG analysis showed the top 10 metabolic pathways with the most significant enrichment of differential metabolites in lung tissue.

system cells.[20] The present study finds that glutamine levels are reduced in the simulated lunar dust group compared with the control group, which may lead to impaired immune cell function, greatly exacerbating disease and infection, prompting inflammatory responses, and causing lung damage. Glutamine entering the cell is deaminated in the mitochondria by GLS to form glutamate, which undergoes glutamate dehydrogenase (GLUD) to form α-ketoglutarate (α-KG) and NADH/NADPH, enter the TCA cycle and regulate intracellular redox homeostasis.[28] Decreased glutamate levels and altered GLS, GDH, GAD, and OGDH activities and Abnormal mRNA expression levels indicate that the TCA cycle is disturbed. It is well known that valine and leucine are branched-chain amino acids that are mainly involved in energy metabolism. In this experiment, the content of valine and leucine decreased, and the disorder of branched-chain amino acid metabolism further indicated that simulated lunar dust exposure accelerated the TCA cycle and energy consumption process, indicating that simulated lunar dust exposure interfered with energy metabolism.

Numerous studies have shown that aspartic acid (Asp) has many important biological metabolic effects. It not only acts as an excitatory amino acid in the central and peripheral nervous systems and participates in the regulation of neural activity, but also is the precursor for the synthesis of various amino acids such as arginine and threonine, as well as purine and pyrimidine, it also participates in various metabolic pathways such as the tricarboxylic acid cycle and urea cycle of the body, and plays an important role in the proliferation of immune cells and the regulation of the immune system.[29] Asparagine (Asn) is a neutral amino acid. In addition to participating in energy metabolism and enhancing the body's metabolism under aerobic conditions, it also plays an important role in regulating the body's immune function,

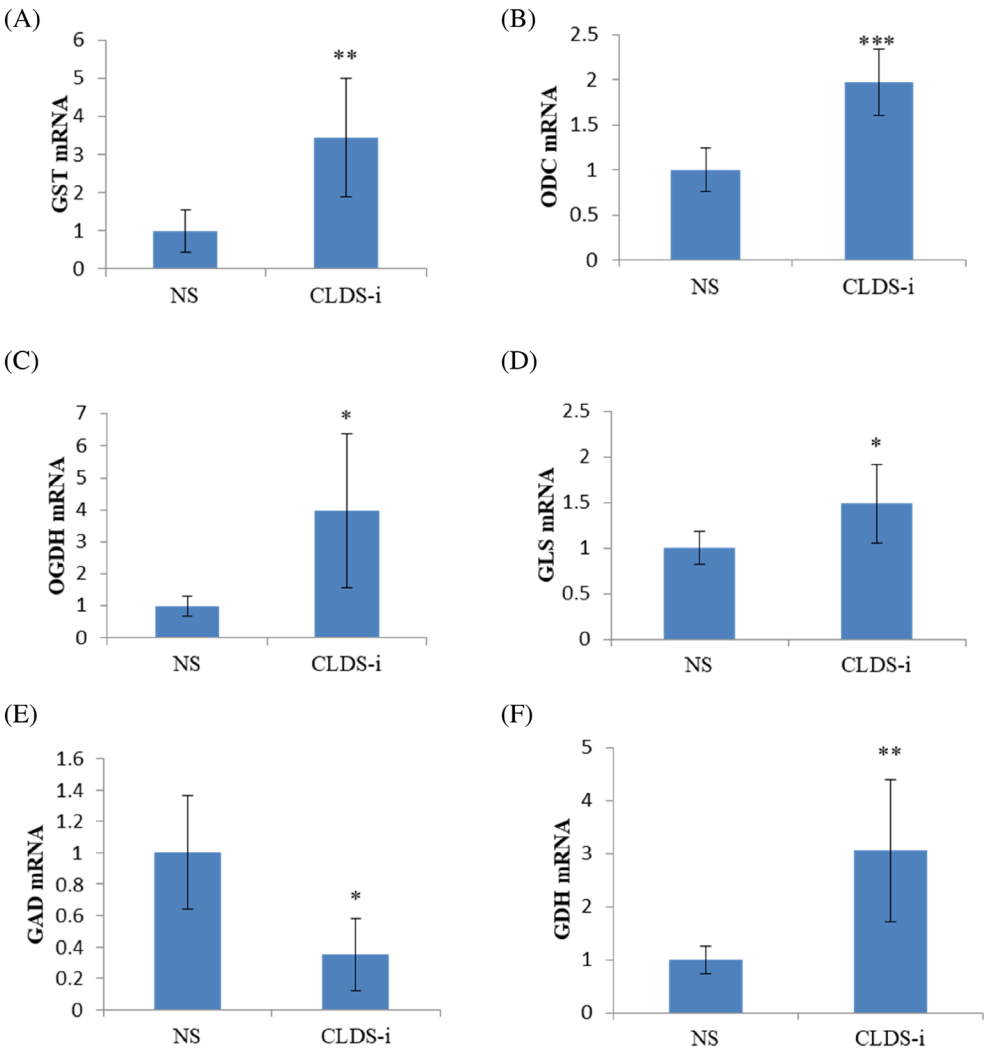

FIGURE 10 GST, ODC, OGDH, GLS, GAD and GDH mRNA expression in rat lungs ($n = 6$). (A) GST mRNA expression. (B) ODC mRNA expression. (C) OGDH mRNA expression. (D) GLS mRNA expression. (E) GAD mRNA expression. (F) GDH mRNA expression. The datum is presented as the means ± SD. Compared with the saline control group, $^{*}p < .05$; $^{**}p < .01$; $^{***}p < .001$.

TABLE 3 The levels of various biochemical indexes in the lung tissue of rats after infection ($n = 4$).

Group	NADH-GDH (nmol/min/g)	GST (nmol/min/g)	GAD (mol/h/g)	GLS (ng/mL)	ODC (ng/mL)	OGDH (g/mL)
NS	119.41 ± 12.56	12.42 ± 6.39	10.66 ± 1.22	32.21 ± 1.38	5.38 ± 0.22	42.66 ± 2.65
CLDS-i	136.88 ± 12.34*	20.46 ± 3.02**	4.41 ± 0.93	35.65 ± 1.53	6.00 ± 0.16	46.59 ± 1.11

Note: Compared with the saline control group.
$^{*}p < .05$; $^{**}p < .01$;$^{***}p < .001$.

especially regulating the immune barrier function of the intestinal mucosa.[30,31] We found that the levels of aspartic acid and asparagine in the lung tissue of the rats in the simulated lunar dust group were decreased, which further indicated that the function of the immune system of the rats was damaged, and the simulated lunar dust disturbed the immune regulation process of the body. Other amino acids, such as histidine and tryptophan, were down-regulated in the simulated lunar dust group compared with the control group in this experiment, while histidine and tryptophan have anti-inflammatory and antioxidant effects and play an important role in inflammatory diseases. Previous studies have shown that histidine supplementation may exert an anti-inflammatory effect by inhibiting the expression of pro-inflammatory factors in adipocytes through the NF-κB pathway.[32] And tryptophan has been shown to be associated with inflammatory bowel disease activity.[33] In addition, lysine metabolism is not only closely related to the function of animal monocyte–macrophage system.[34] It is also one of the important energy sources. Affects the synthesis of bone collagen and regulates bone metabolism.[35] In this experiment, the lysine level in lung tissues of rats of the simulated lunar dust group was reduced, further indicating that this fine particulate matter affected the body's energy metabolism pathway. In addition, the reduction of taurine levels in the lung tissue of rats in the simulated lunar dust group confirmed that oxidative stress is the basic biological effect of simulated lunar dust exposure. According to reports, taurine, also known as β-aminoethanesulfonic acid, has strong antioxidant activity, can effectively remove most of the oxygen free

radicals in the body, and has many effects such as inhibiting lipid peroxidation and reducing tissue oxygen consumption.[36] Therefore, taurine is widely regarded as a potent free radical scavenger. It has been reported that taurine can inhibit the reactive oxygen species (ROS) by ameliorating mitochondrial dysfunction, thereby attenuating ionizing radiation-induced renal injury.[37] Researchers also found that taurine can improve blood sugar and blood lipid metabolism in diabetes,[38] but it has not been elucidated whether taurine improves glucose and lipid metabolism by regulating oxidative stress.

Oxidant/antioxidant imbalance is a major cause of cellular damage and a hallmark of lung inflammation.[28] Glutathione (GSH), a ubiquitous tripeptide thiol, is an important intracellular and extracellular antioxidant against oxidative stress and plays a key role in controlling signaling and proinflammatory processes in the lung.[39] The lungs are one of the main sources of glutathione storage.[39] Low levels of GSH may lead to an imbalance between oxidants and antioxidants in lung tissue, enhancing inflammatory responses and worsening lung damage. Glutathione levels were elevated in this study, which is different from our previous findings.[5] We speculate that the pattern and duration of simulated lunar dust exposure may have been different in the studies, causing this discrepancy. It is generally believed that depletion of GSH in tissue cells in the initial stage of oxidative stress reduces the level of GSH, and then due to the feedback regulation of GSH and the stimulation of internal and external oxides, the expression of γ-GCS gene in the airway wall and lung epithelial cells is enhanced, and the synthesis of GSH is increased. And activation, resulting in increased levels of GSH and increased antioxidant capacity in the lungs to adapt to a sustained oxidative state.[40] In addition, a large body of literature indicates that GSH levels are different in different inflammatory lung diseases. Its mechanism is unclear. For example, GSH is reduced in idiopathic pulmonary fibrosis, ARDS, cystic fibrosis, lung allograft patients, and HIV+ patients.[41–45] In contrast, patients with mild asthma have higher total GSH concentrations in the bronchial and alveolar fluids.[46] Rahman et al suggested that differences in glutathione in various inflammatory lung diseases may be due to changes in the molecular regulation of GSH synthesis in lung cells.[39] Afterwards, we detected the activity and mRNA level of GST, an important antioxidant enzyme in animals. Compared with the control group, the enzyme activity and mRNA expression of GST were significantly increased. It is suggested that simulated lunar dust induces oxidative stress in rat lung tissue and leads to the increase of GST activity, and the increase of GST activity is the response of the body to oxidative stress. In conclusion, the changes of GSH levels and GST indicate that the oxidative/antioxidative state of the body is disordered, which induces infection and inflammation, and makes the lung disease gradually develop and worsen.

The UPLC-MS metabolomic approach in our study also revealed changes in arginine and polyamine metabolism. We found that compared with the control group, the level of arginine and spermidine in the lung tissue of rats in the simulated lunar dust group was decreased. Arginine is an essential nitrogen carrier for the synthesis of urea, polyamines, proline and other proteins in healthy adults, has immunomodulatory activity and can reduce inflammatory responses.[47] In the body, L-arginine is the only precursor for endogenous nitric oxide.[48] Under the activation of the Arg-NO pathway, NO is catalytically generated. Some literature show that NO can inhibit the secretion of TNF-α, and supplementation of L-arginine can increase the secretion of glucagon-like peptide-1 (GLP-1), which in turn stimulates the secretion of glucagon-like peptide-1 (GLP-1). NO production increases and inhibits the nuclear factor (NF)-κB pathway, while indirectly inhibiting the secretion of inflammatory cytokines such as TNF-α to suppress the inflammatory response.[49] Murakami et al. found that arginine supplementation to sheep inhaled by burns and smoke significantly improved gas exchange and lung function, and alleviated lung damage in animals caused by burns and smoke.[50] In experiments examining the effects of arginine supplementation on septic mice, it was found that arginine supplementation down-regulated the production of inflammatory cytokines in lung tissue and reduced lung tissue damage.[47] Additionally, arginine was found to improve antioxidant capacity in male rats.[51] A large numbers of animal studies have shown that arginine can effectively inhibit the body's oxidative stress and induce endogenous antioxidant processes, and inhibit the expression of inflammatory factors, thereby improving lung injury. Polyamines are a class of aliphatic amines that are widely present in all living organisms. Spermidine is a type of polyamine. Because polyamines can interact with DNA, ATP, phospholipids, and certain kinds of proteins,[52] polyamines are essential for cellular metabolism, growth, and tissue turnover.[53] Ornithine decarboxylase catalyzes the decarboxylation of ornithine and is the first rate-limiting enzyme in polyamine synthesis and plays an important role in regulating cell proliferation and apoptosis.[54–56]A large number of literature show that the changes of ODC expression levels are closely related to the occurrence of tumors. Therefore, ODC determination is of great significance in the early diagnosis of tumors and is considered as a new target for anti-tumor therapy. In this study, the polyamine levels in the simulated lunar dust group were significantly decreased, and the changes in ODC activity and its mRNA levels indicated that the exposure of simulated lunar dust may affect many cellular biological processes, such as cell growth, proliferation, division and differentiation may be disordered.

There are still some limitations to our study. Since the study was conducted on Earth, this is different from what astronauts are exposed to the real environment. This difference is predicted to make the lunar dust more toxic. In future studies, we need to pay more attention to the metabolic effects caused by lunar dust exposure at different times, identify the specific components of lunar dust in the lunar surface environment that produce toxic effects, and determine the specific role of these metabolic changes in the pathogenesis caused by lunar dust exposure. The internal relationship between final metabolites and related genes was elucidated by combining genomics and transcriptomics. Multi-omics analysis can further reveal the effect of lunar dust exposure on body metabolism.

5 | CONCLUSION

In the present study, metabolite changes in the lung tissues of rats treated with simulated lunar dust CLDS-i were analyzed by a metabolic approach using UPLC-MS. The results of metabolic analysis showed that 141 metabolites were significantly changed in CLDS-i-treated lung tissue, mainly involving amino acid metabolism, lipid metabolism and nucleotide metabolism, indicating that CLDS-i exposure caused the metabolism of these substances to occur disorder. Combined with metabolic pathway analysis, amino acid metabolism had the greatest impact. Significant changes in the activities of six key enzymes of amino acid metabolism were measured, as well as abnormal mRNA expression of these key enzymes, which also indicated that CLDS-i significantly disturbed the balance of amino acid metabolism in lung tissue.

AUTHOR CONTRIBUTIONS

Chen Gu performed the experiments, analyzed the data, and wrote the manuscript. Yan Sun designed the study, review and supervision. Yuhang Yin performed the experiments. Jinguo Liu contributed to the design of the study, review and editing. Xiongyao Li review, editing and supervision. Xiaoping Zhang review and editing. All authors have read and agreed to the published version of the manuscript.

ACKNOWLEDGMENTS

This study was supported by the Doctoral Scientific Research Fund of Liaoning Provincial Science and Technology Department (20198023), Open Projects Funding of Lunar and Planetary Science Laboratory, MUST—Partner Laboratory of Key Laboratory of Lunar and Deep Space Exploration, CAS (Macau FDCT grant No. 119/2017/A3), the Science and Technology Development Fund (FDCT) of Macau (0014/2022/A1), and the Science and Technology Research Fund of Shenyang Medical College (20191017).

CONFLICT OF INTEREST STATEMENT

The authors declare no conflict of interest.

DATA AVAILABILITY STATEMENT

No data was used for the research described in the article.

ORCID

Chen Gu https://orcid.org/0000-0002-0241-3197

REFERENCES

1. Sun Y, Zhang L, Liu J, et al. Effects of lunar dust simulant on cardiac function and fibrosis in rats. *Toxicol Res*. 2019;8:499-508.
2. Lam CW, James JT, Latch JN, Holian A. Pulmonary toxicity of simulated lunar and Martian dusts in mice: II. Biomarkers of acute responses after intratracheal instillation. *Inhal Toxicol*. 2002;14:917-928.
3. Lam CW, James JT, McCluskey R, Cowper S, Balis J, Muro-Cacho C. Pulmonarytoxicity of simulated lunar and Martian dusts in mice: I. histopathology 7 and 90 days after intratracheal instillation. *Inhal Toxicol*. 2002;14:901-916.
4. Sun Y, Liu JG, Zheng YC, et al. Research on rat's pulmonary acute injury induced by lunar soil simulant. *J Chin Med Assoc*. 2018;81:133-140.
5. Sun Y, Liu JG, Di KY, et al. Effects of lunar soil simulant on systemic oxidative stress and immune response in acute rat lung injury. *Int J Pharmacol*. 2018;14:766-772.
6. Sun Y, Liu J, Zhang X, Li X, Zhou B, Lv Z. Mechanisms involved in inflammatory pulmonary fibrosis induced by lunar dust simulant in rats. *Environ Toxicol*. 2019;34:131-140.
7. Li J, Hu Y, Liu L, Wang Q, Zeng J, Chen C. $PM_{2.5}$ exposure perturbs lung microbiome and its metabolic profile in mice. *Sci Total Environ*. 2020;721:137432.
8. Wang X, Jiang S, Liu Y, et al. Comprehensive pulmonary metabolome responses to intratracheal instillation of airborne fine particulate matter in rats. *Sci Total Environ*. 2017;592:41-50.
9. Huang D, Zou Y, Abbas A, Dai B. Nuclear magnetic resonance-based metabolomic investigation reveals metabolic perturbations in $PM_{2.5}$-treated A549 cells. *Environ Sci Pollut Res Int*. 2018;25:31656-31665.
10. Li R, Peng X, Wu Y, et al. Exposure to $PM_{2.5}$ during pregnancy causes lung inflammation in the offspring: mechanism of action of mogrosides. *Ecotoxicol Environ Saf*. 2021;228:112955.
11. Zhang SY, Shao DQ, Liu HY, et al. Metabolomics analysis reveals that benzo[a]pyrene, a component of PM2.5, promotes pulmonary injury by modifying lipid metabolism in a phospholipase A2-dependent manner in vivo and in vitro. *Redox Biol*. 2017;13:459-469.
12. Subacute inhalation toxicology: 28-day study, OECD guidelines for the testing of chemicals. OECD. 2018 Test No. 412.
13. Szapiel SV, Elson NA, Fulmer JD, et al. Bleomycin-induced interstitial pulmonary disease in the nude, athymic mouse. *Am Rev Respir Dis*. 1979;120:893-899.
14. Hou L, Guan S, Jin Y, et al. Cell metabolomics to study the cytotoxicity of carbon black nanoparticles on A549 cells using UHPLC-Q/TOF-MS and multivariate data analysis. *Sci Total Environ*. 2020;698:134122.
15. Ting L, Cowley MJ, Hoon SL, Guilhaus M, Raftery MJ, Cavicchioli R. Normalization and statistical analysis of quantitative proteomics data generated by metabolic labeling. *Mol Cell Proteomics*. 2009;8:2227-2242.
16. Lam CW, Scully RR, Zhang Y, et al. Toxicity of lunar dust assessed in inhalation-exposed rats. *Inhal Toxicol*. 2013;25:661-678.
17. Wu G. Amino acids: metabolism, functions, and nutrition. *Amino Acids*. 2009;37:1-17.
18. Cruzat V, Macedo Rogero M, Noel Keane K, et al. Glutamine: metabolism and immune function supplementation and clinical translation. *Nutrients*. 2018;10:1564.
19. Curi R, Lagranha CJ, Doi SQ, et al. Molecular mechanisms of glutamine action. *J Cell Physiol*. 2005;204:392-401.
20. Curi R, Newsholme P, Marzuca-Nassr GN, et al. Regulatory principles in metabolism-then and now. *Biochem J*. 2016;473:1845-1857.
21. Cruzat VF, Pantaleão LC, Donato J, de Bittencourt PIH, Tirapegui J. Oral supplementations with free and dipeptide forms of L-glutamine in endotoxemic mice: effects on muscle glutamine-glutathione axis and heat shock proteins. *J Nutr Biochem*. 2014;25:345-352.
22. Raizel R, Leite JS, Hypólito TM, et al. Determination of the anti-inflammatory and cytoprotective effects of l-glutamine and l-alanine, or dipeptide, supplementation in rats submitted to resistance exercise. *Br J Nutr*. 2016;116:470-479.
23. Singleton KD, Wischmeyer PE. Glutamine attenuates inflammation and NF-kappaB activation via Cullin-1 deneddylation. *Biochem Biophys Res Commun*. 2008;373:445-449.
24. Zabot GP, Carvalhal GF, Marroni NP, Hartmann RM, da Silva VD, Fillmann HS. Glutamine prevents oxidative stress in a model of mesenteric ischemia and reperfusion. *World J Gastroenterol*. 2014;20:11406-11414.

25. Newsholme P. Why is L-glutamine metabolism important to cells of the immune system in health, postinjury, surgery or infection? *J Nutr*. 2001;131:2514S-2523S.
26. Cruzat VF, Krause M, Newsholme P. Amino acid supplementation and impact on immune function in the context of exercise. *J Int Soc Sports Nutr*. 2014;11:61.
27. Rodas PC, Rooyackers O, Hebert C, Norberg Å, Wernerman J. Glutamine and glutathione at ICU admission in relation to outcome. *Clin Sci (Lond)*. 2012;122:591-597.
28. Geck RC, Toker A. Nonessential amino acid metabolism in breast cancer. *Adv Biol Regul*. 2016;62:11-17.
29. Wu G, Bazer FW, Davis TA, et al. Important roles for the arginine family of amino acids in swine nutrition and production. *Livest Sci*. 2007;112:8-22.
30. Marquezi ML, Roschel HA, dos Santa Costa A, et al. Effect of aspartate and asparagine supplementation on fatigue determinants in intense exercise. *Int J Sport Nutr Exerc Metab*. 2003;13:65-75.
31. Li P, Yin YL, Li D, Woo Kim S, Wu G. Amino acids and immune function. *Br J Nutr*. 2007;98:237-252.
32. Feng RN, Niu YC, Sun XW, et al. Histidine supplementation improves insulin resistance through suppressed inflammation in obese women with the metabolic syndrome: a randomised controlled trial. *Diabetologia*. 2013;56:985-994.
33. Schicho R, Storr M. IBD: patients with IBD find symptom relief in the cannabis field. *Nat Rev Gastroenterol Hepatol*. 2014;11:142-143.
34. Calder P, Buttriss J. Nutrition and immune system. *Encyclopedia of Immunology*. 2001;52:1869-1871.
35. Hall SL, Greendale GA. The relation of dietary vitamin C intake to bone mineral density: results from the PEPI study. *Calcif Tissue Int*. 1998;63:183-189.
36. Maleki V, Mahdavi R, Hajizadeh-Sharafabad F, Alizadeh M. The effects of taurine supplementation on oxidative stress indices and inflammation biomarkers in patients with type 2 diabetes: a randomized, double-blind, placebo-controlled trial. *Diabetol Metab Syndr*. 2020;12:9.
37. Ma N, Kato T, Isogai T, et al. The potential effects of taurine in mitigation of radiation nephropathy. *Adv Exp Med Biol*. 2019;1155:497-505.
38. Sarkar P, Basak P, Ghosh S, Kundu M, Sil PC. Prophylactic role of taurine and its derivatives against diabetes mellitus and its related complications. *Food Chem Toxicol*. 2017;110:109-121.
39. Rahman I. Regulation of glutathione in inflammation and chronic lung diseases. *Mutat Res*. 2005;579:58-80.
40. Ray S, Watkins DN, Misso NL, et al. Oxidant stress induces gammaglutamylcysteine synthetase and glutathione synthesis in human bronchial epithelial NCI-H292 cells. *Clin Exp Allergy*. 2002;32:571-577.
41. Buhl R, Jaffe HA, Holroyd KJ, et al. Systemic glutathione deficiency in symptom-free HIV-seropositive individuals. *Lancet*. 1989;2:1294-1298.
42. Cantin AM, Hubbard RC, Crystal RG. Glutathione deficiency in the epithelial lining fluid of the lower respiratory tract in idiopathic pulmonary fibrosis. *Am Rev Respir Dis*. 1989;139:370-372.
43. Baz MA, Tapson VF, Roggli VL, van Trigt P, Piantadosi CA. Glutathione depletion in epithelial lining fluid of lung allograft patients. *Am J Respir Crit Care Med*. 1996;153:742-746.
44. Bunnell E, Pacht ER. Oxidized glutathione is increased in the alveolar fluid of patients with the adult respiratory distress syndrome. *Am Rev Respir Dis*. 1993;148:1174-1178.
45. Roum JH, Buhl R, McElvaney NG, et al. Systemic deficiency of glutathione in cystic fibrosis. *J Appl Physiol*. 1985;1993(75):2419-2424.
46. Smith LJ, Houston M, Anderson J. Increased levels of glutathione in bronchoalveolar lavage fluid from patients with asthma. *Am Rev Respir Dis*. 1993;147:1461-1464.
47. Yeh CL, Pai MH, Shih YM, Shih JM, Yeh SL. Intravenous arginine administration promotes proangiogenic cells mobilization and attenuates lung injury in mice with polymicrobial sepsis. *Nutrients*. 2017;9:507.
48. Alimohammadi S, Zendehdel M, Babapour V. Modulation of opioid-induced feeding behavior by endogenous nitric oxide in neonatal layer-type chicks. *Vet Res Commun*. 2015;39:105-113.
49. Liao SY, Linderholm A, Showalter MR, Chen CH, Fiehn O, Kenyon NJ. L-arginine as a potential GLP-1-mediated immunomodulator of Th17-related cytokines in people with obesity and asthma. *Obes Sci Pract*. 2021;7:339-345.
50. Murakami K, Enkhbaatar P, Yu YM, et al. L-arginine attenuates acute lung injury after smoke inhalation and burn injury in sheep. *Shock*. 2007;28:477-483.
51. Silva EP Jr, Borges LS, Mendes-da-Silva C, Hirabara SM, Lambertucci RH. L-arginine supplementation improves rats' antioxidant system and exercise performance. *Free Radic Res*. 2017;51:281-293.
52. Igarashi K, Kashiwagi K. Modulation of cellular function by polyamines. *Int J Biochem Cell Biol*. 2010;42:39-51.
53. Pegg AE. Functions of polyamines in mammals. *J Biol Chem*. 2016;291:14904-14912.
54. Pegg AE, PP MC. Polyamine metabolism and function. *Am J Physiol*. 1982;243:C212-C221.
55. Thomas T, Thomas TJ. Polyamine metabolism and cancer. *J Cell Mol Med*. 2003;7:113-126.
56. Grimminger PP, Schneider PM, Metzger R, et al. Ornithine decarboxylase mRNA expression in curatively resected non-small-cell lung cancer. *Clin Lung Cancer*. 2010;11:114-119.

How to cite this article: Gu C, Yin Y, Sun Y, Liu J, Li X, Zhang X. Exploring the mechanism of lung injury induced by lunar dust simulant in rats based on metabolomic analysis. *Environmental Toxicology*. 2024;39(1):184-198. doi:10.1002/tox.23967